Detecting scaling in the period dynamics of multimodal signals: Application to Parkinsonian tremor

Nir Sapir,[1] Roman Karasik,[1] Shlomo Havlin,[1] Ely Simon,[2] and Jeffrey M. Hausdorff[2,3]

[1]*Department of Physics and Gonda-Goldschmied Medical Diagnostic Research Center, Bar-Ilan University, Ramat-Gan 52900, Israel*
[2]*Movement Disorders Unit, Tel-Aviv Sourasky Medical Center, Tel-Aviv, Israel*
[3]*Gerontology Division, Beth Israel Deaconess Medical Center, Boston, Massachusetts 02215*

Patients with Parkinson's disease exhibit tremor, involuntary movement of the limbs. The frequency spectrum of tremor typically has broad peaks at ''harmonic'' frequencies, much like that seen in other physical processes. In general, this type of harmonic structure in the frequency domain may be due to two possible mechanisms: a nonlinear oscillation or a superposition of (multiple) independent modes of oscillation. A broad peak spectrum generally indicates that a signal is semiperiodic with a fluctuating period. These fluctuations may posses intrinsic order that can be quantified using scaling analysis. We propose a method to extract the correlation (scaling) properties in the period dynamics of multimodal oscillations, in order to distinguish between a nonlinear oscillation and a superposition of individual modes of oscillation. The method is based on our finding that the information content of the temporal correlations in a fluctuating period of a single oscillator is contained in a finite frequency band in the power spectrum, allowing for decomposition of modes by bandpass filtering. Our simulations for a nonlinear oscillation show that harmonic modes possess the same scaling properties. In contrast, when the method is applied to tremor records from patients with Parkinson's disease, the first two modes of oscillations yield different scaling patterns, suggesting that these modes may not be simple harmonics, as might be initially assumed.

I. INTRODUCTION

The presence of scaling and long-range correlations in a wide variety of physical [1–3], biological [4–6], meteorological [7], and economic [8,9] systems has recently attracted much interest. The appearance of scaling laws is generally associated with the complex, nonequilibrium nature of a system, especially where continuous flow, dissipation of energy, and feedback loops are present [10]. Biological systems often have these characteristics since they feature complex environments with a large number of units interacting locally and nonlinearly and include multiple, natural pacemakers as well as feedback mechanisms [11]. Such interactions may lead to nonlinearity and higher harmonics. Recent studies have focused on identifying long-range temporal correlations in phenomena that fluctuate with a certain rhythm or periodicity, but in which the frequency is not constant in time, e.g., heartbeat dynamics [12,13], human gait [14], and neuron spiking [15]. In such systems, the semiperiodic signal (not perfectly periodic) possesses long-range correlations inside its period dynamics (the time series constructed by the evolution of the instantaneous period). To determine whether long-range correlations exist in the nonconstant frequency of a measured quantity, one first needs to decide what to consider as the instantaneous period. When dealing with rhythmic signals, one usually encounters a typical frequency of oscillation and therefore the time-dependent period can readily be defined as the time interval between successive peaks. The period in this manner, however, may be sometimes ill defined, e.g., when the oscillation is the product of several typical frequencies, and not just one.

Many patients with Parkinson's disease exhibit pathological tremor, a movement disorder that results from the involuntary fluctuations of a limb. This motion is neither strictly periodic nor is it made up of only one oscillation mode (frequency band), a property common to many physical and physiological signals. Tremor can be quantified by measuring the acceleration or muscle activity of the hand; both reveal a semiperiodic wave form with more than one typical frequency (Fig. 1). There are (at least) two possible explanations for the appearance of a multimodal spectrum in the
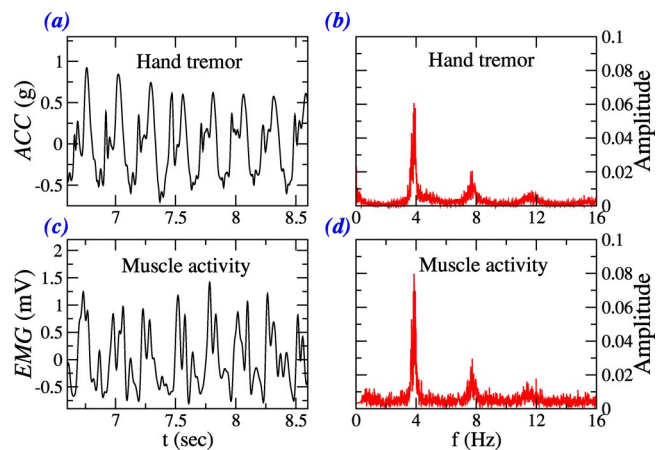

FIG. 1. Example of hand tremor (a) and muscle activity (c) from a patient with Parkinson's disease, and corresponding power spectra (b) and (d). The spectra reveal several modes, apparently at harmonic frequencies, which may rise from the nonlinear nature of the signal. Another option is that they may actually indicate different, perhaps independent modes of oscillation. Note that for both hand tremor and muscle activity, the peaks appear at the same frequencies.

frequency domain. One is that the oscillation has only one typical period, but it is of nonlinear nature. In this case, there is only one statistical "origin" for the period dynamics. Since the signal is semiperiodic, nonsinusoidal, it generates harmonic structure in the power spectrum. The second is that the oscillation is described by coexisting modes that may have different statistical origins. The individual modes may possess statistically independent behavior, as expressed in the period dynamics. The apparent "harmonic" relation between the modes may not be a mere coincidence, but can be attributed to a certain system that allows only harmonic modes to exist, e.g., a chain of coupled oscillators with modes at ratios of 1:1, 1:2, or 1:4, for example, or a feedback loop. Thus, the signal that produces the multimodal harmonic structure may be either a linear combination of oscillator eigenmodes, or a single nonlinear oscillator.

Previous studies have begun to investigate whether the different frequencies indicate a single nonlinear oscillator or superimposed, multiple biological oscillators [16,17]. For example, they may represent multiple tremor mechanisms that may include central oscillations, peripheral feedback loops, and mechanical resonance [18]. To gain insight into the origins of tremor and the mechanisms responsible for the generation of different modes, we would like to quantitatively characterize the time evolution of the fluctuating period using scaling analysis (see the Appendix). Scaling usually appears in long-term memory processes, such as fractal brownian motion, and is associated with $1/f$ noise. The harmonic or quasiharmonic signals themselves do not posses scaling properties, however, the time series of their fluctuating periods may (e.g., as in heart rate dynamics). But first, in order to obtain the period series of tremor signals, we need to separate the different oscillation modes. Simple splines that rid the signal from noise and other high frequencies cannot be used [19]. Therefore, in order to enable scaling analysis of tremor, specifically, and signals consisting of several modes, more generally, it is essential to develop a new method for identifying the period dynamics of individual modes in a multimodal signal. As we show below, subsequent investigation of the scaling properties of the decomposed individual modes will, in turn, provide important evidence regarding the question of whether the multiple modes are simply harmonics that arise from a single, nonlinear oscillator or whether they are likely to be the result of distinct oscillators.

II. METHODS

Two assumptions lie at the basis of our method. The first is that independent processes may be responsbile for different correlation (scaling) properties inside the period dynamics of individual modes of oscillation. The second is that the output signal is a superposition of modes, even if those arise from a single nonlinear oscillation. A consequence of the two assumptions is that the period dynamics can be recovered independently for each of the modes. We propose to decompose the multimode signal into its subsignals using a filtering procedure, in order to extract scaling information about the period dynamics of different modes. We hypothesize that even if the period dynamics of each oscillator possess long-

range correlations, i.e., no characteristic time scale, its dynamical properties may be contained in a finite frequency band located around the central frequency and not spread over the entire spectrum. Therefore, if several modes with a variety of dynamics are present, one can apply a filter in the frequency domain in a bandpass fashion to identify the long-range temporal correlations inside the fluctuating period, for each mode separately, disregarding any low-frequency components. Perhaps this idea is counterintuitive; long-term memory is typically associated with low-frequency contributions. Here, however, we discuss memory in the period dynamics and demonstrate that this memory is reflected only in the vicinity of the peak. Another point to be examined with respect to bandpass filtering is the possible mixing of statistical properties at different times, which might therefore disable the time ordering that is cruical for scaling. In the following, we demonstrate that this does not occur. When two different filters are applied, similar scaling is observed.

A. Simulation procedure

To test our method, we first simulate a single-mode signal that has long-range correlations in its period dynamics, but has a constant amplitude. We generate a Gaussian distributed correlated noise series $\{\eta_i\}$ [20] and determine the series of the periods as

$$T_i = \bar{T} + \eta_i. \tag{1}$$

Sinusoids with a fluctuating period T_i are created one after another. As soon as one wave completes its period, another is created. Thus we have a distribution of sinusoids with different periods T_i. The period dynamics of these sinusoids are the same as that of the correlated noise series, $\{\eta_i\}$. The analytical representation of such a superposition of delayed finite-duration sinusoids can be written as

$$y(t) = \sum_{i=1}^{N} \cos\left[\frac{2\pi}{T_i}\left(t - \sum_{j=0}^{i-1} T_j\right)\right] \theta\left(t - \sum_{j=0}^{i-1} T_j\right)$$
$$\times \theta\left(\sum_{j=0}^{i} T_j - t\right), \tag{2}$$

where N is the number of sinusoids in the signal $y(t)$ (or the length of the period series $\{T_i\}$), and

$$\theta(t) = \begin{cases} 0, & t < 0 \\ 1, & t \geq 0. \end{cases}$$

The Fourier transform of this function can be estimated using some basic properties. We define the transform pair of the function $h(t)$ as [21]

$$h(t) \Leftrightarrow H(\omega) = \frac{1}{2\pi} \int_{-\infty}^{\infty} h(t) \exp(i\omega t) dt. \tag{3}$$

Then using "time shifting" and "modulation" we obtain Eqs. (4) and (5), respectively,

$$h(t - t_0) \Leftrightarrow H(\omega) \exp(i\omega t_0), \tag{4}$$

$$h(t)\cos(\omega_0 t) \Leftrightarrow \frac{1}{2}[H(\omega - \omega_0) + H(\omega + \omega_0)]. \qquad (5)$$

The transform pair of a square pulse with a width T centered around $t = 0$,

$$\theta\left(t + \frac{T}{2}\right)\theta\left(\frac{T}{2} - t\right) \Leftrightarrow \frac{T}{2\pi}\frac{\sin\left(\frac{\omega T}{2}\right)}{\frac{\omega T}{2}}. \qquad (6)$$

It is more convenient to look only at the first term of the Fourier transform for Eq. (2), because the second term is simply the complex conjugate of the reflected first term. Thus, $y(t) \Leftrightarrow Y(\omega) = G(\omega) + G^*(-\omega)$. Using Eqs. (4)–(6), we obtain

$$G(\omega) = \frac{1}{2}\sum_{n=1}^{N}\frac{T_n}{2\pi}\frac{\sin\left[(\omega - \omega_n)\frac{T_n}{2}\right]}{(\omega - \omega_n)\frac{T_n}{2}}\exp[i(\omega - \omega_n)\tau_n],$$

$$(7)$$

where

$$\omega_n \equiv \frac{2\pi}{T_n} \qquad \text{and} \qquad \tau_n \equiv T_n/2 + \sum_{j=0}^{n-1}T_j.$$

From Eq. (7), we can see that if $\{T_i\}$ is a series centered around a central period, then in the Fourier transform only values in the vicinity of that period are important; the function decays without low-frequency contribution as $1/(\omega - \omega_n)$, even if long-range memory is present in the period series $\{T_i\}$. Such memory is determined only in the amplitude and phase distribution around the central period, so the signal, to some extent, is bandwidth limited. The power spectrum of the simulated single-mode oscillator indeed reveals a broad peak located around the central frequency (Fig. 2). Although the phase is not zero outside the broad peak, the information content carried there is minimal, since the corresponding amplitudes are effectively nil.

B. Robustness of the method

To test whether a filtering procedure can correctly recover long-range correlations in the period dynamics of the simulated signals, we superimpose two single-mode oscillators to construct a double-mode oscillator. This double-mode signal, a prototype for our decomposition trial [Fig. 2(a)], is then just the linear combination of the two single-mode signals, $f(t) = y_1(t) + y_2(t)$, with different central periods $\bar{T}_1$ and $\bar{T}_2$, respectively, and different noise series, η_1 and η_2, characterized by different scaling exponents α_1 and α_2. We choose $\bar{T}_1 = 2\bar{T}_2$ and denote $y_1(t)$ as the first mode and $y_2(t)$ as the second mode, to produce a harmonic structure. To switch to the frequency domain, the Fourier transform of the double-mode signal is calculated [Fig. 2(b)]. Then a pair of bandpass filters are applied to the double-mode signal in order to de-
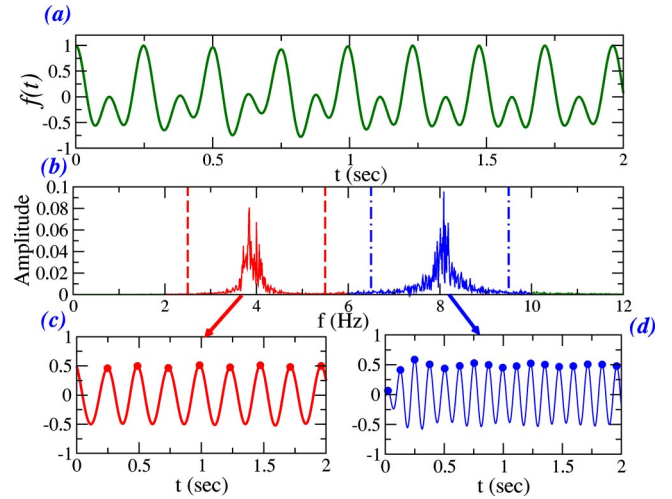

FIG. 2. Simulation for the validation of bandpass filtering decomposition of a double-mode signal. (a) The linear combination of two single-mode signals, with altering periods; one sinusoid has a cycle centered around 0.25 sec and the second at 0.125 sec. The two sinusoids may have different scaling exponents describing the dynamics of the periods. (b) Power spectrum of the simulated signal presented in (a), showing two broad peaks at the corresponding central frequencies. We decompose the signal into the two modes with a bandpass filter whose boundaries are indicated by dashed lines for the first mode and by dot-dashed lines for the second mode. The decomposed subsignals for the first mode and for the second mode are shown in (c) and (d), respectively.

compose it into its subsignals (for the first and second mode). We use a square pulse filter, which conserves the magnitude and phase information inside a chosen bandwidth and discards all information content outside the band. Afterwards, the inverse Fourier transforms of the results are estimated to switch back to the time domain for peak detection [Figs. 2(c) and 2(d)]. The period dynamics of the decomposed subsignals for the two modes is determined from the peak-to-peak intervals (PPI) series—the intervals between successive maxima. Similiar results were obtained when a Blackman filter, which decays more slowly, was applied instead of the square pulse filter. This consistency suggests that, at least to some degree, the method is independent of the filter shape. We chose to use the square pulse filter since its results can be more intuitively explained.

The correlation properties of the PPI series for both modes are then investigated using detrended fluctuation analysis (DFA) [22,23]. DFA calculates the fluctuation function of a time series, which in the case of long-range correlations behaves as a power law of time scales [24], $F(n) \sim n^\alpha$. When the scaling exponent α is larger, it indicates stronger correlations in the signal (for more details see the Appendix). The fluctuation functions of the PPI series of the decomposed subsignals are compared with the fluctuation function of the PPI series of the original single-mode signal to see whether the method is able to restore the correct, original scaling exponent. In Fig. 3, it is apparent that the correlation properties of the decomposed first mode signal are identical to those of the original single-mode signal, $y_1(t)$, in the large time scales, but there is some deviation in the small
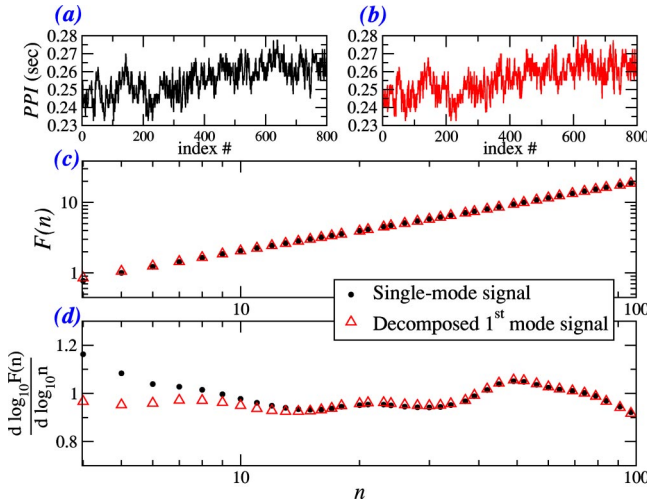
FIG. 3. Detrended fluctuation analysis (DFA) of the peak-to-peak intervals (PPI) for the simulation shown in Fig. 2. (a) The PPI series of the single-mode (input) signal. (b) The PPI series of the decomposed first mode signal. (c) Fluctuation functions of the PPI series of (a) and (b), where "●" indicates DFA results of the single-mode signal, and "△" indicates DFA results of the decomposed first mode signal, obtained by bandpass filtering of the double-mode signal. (d) Successive slopes of the fluctuation functions from (c). The two curves overlap for almost all window sizes, indicating that the decomposition restores the correlations in the PPI series of the single-mode signal. Subtle deviations occur for small n, perhaps to finite bandwidth effects. See the Appendix for details on DFA.

time scales. The same is true for the decomposed second mode signal. This effect may originate from the finite bandwidth. Thus, although the fluctuations of the period possess scale-free behavior, the dynamics can be reconstructed by selecting a finite scale of frequencies when analyzing the signal.

We test the robustness of the decomposition method for a variety of input scaling exponents (Fig. 4) for the period series from Eq. (1) for both the first and second modes. The scaling exponents for the modes are calculated outside the small scale range to prevent incorrect estimation as indicated by Fig. 3(c). The decomposition method produces stable results regardless of the scaling exponent of the other mode. The sensitivity of the technique to different band limits of the square pulse filter is also tested (Fig. 5). The correct scaling exponents that match the input values are consistently recovered, as long as the band limits do not approach the oscillator frequencies. The calculated scaling exponent then acts as an almost smooth function with small fluctuations, but no sharp deviations, and closely matches the input value. As the filtering boundaries approach the actual peaks, the scaling exponent changes drastically and no longer corresponds to the input value.

Therefore, the filtering procedure indeed preserves the correlations and scaling properties of the periods and can be used to extract the dynamical properties of single-mode signals from double- (or multi)mode signals.
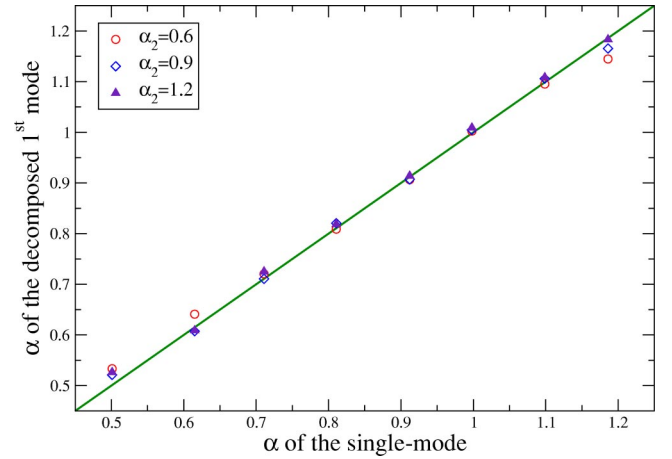

FIG. 4. A comparison between the scaling exponents of the peak-to-peak interval series of the original single-mode signal with the those of the decomposed first mode. Different symbols indicate different input scaling exponents for the period dynamics of the second mode. Note that the decomposition procedure succeeds in restoring the scaling exponent of the single mode, unrelated to the scaling exponent of the second mode. The same picture appears for the second mode, with the scaling exponent of the single mode restored regardless of the scaling exponent of the first mode.

C. Nonlinear oscillation

It is also interesting to see how the method deals with a nonlinear oscillation with long-range correlations in the period. For this purpose, we generate a different oscillating function, a pulse train formed as

$$y(t) = \sum_{i=1}^{N} \delta\left(t - \sum_{j=0}^{i-1} T_j \right), \quad T_i = \bar{T} + \eta_i, \qquad (8)$$

where

$$\delta(t) = \begin{cases} 1, & t = 0 \\ 0, & t \neq 0, \end{cases}$$

to examine the situation where there is only one source for the correlations in a nonlinear signal [Fig. 6(a)]. As in a perfectly periodic pulse train in time that produces a perfectly periodic pulse train in the frequency domain, when fluctuations are introduced to the period, a similar spectrum is produced but with widened peaks [Fig. 6(b)]. The frequencies at which the broad peaks are located are then integer multiples of the basic one. Applying the decomposition method to these harmonic modes, we find that their fluctuation functions perfectly overlap (after normalization by the harmonic number to fit the time scales [25]), showing that the correlation properties of the modes are identical [Fig. 6(c)]. This result can be explained by the fact that it is possible to express this nonlinear oscillation as a linear combination of modes. Then in our case of long-range correlations, each of the modes that make up the sum has the same correlation properties as the nonlinear oscillation, since only one source of correlations exists. This implies that the scaling of the PPI series of harmonic modes originates from the scaling
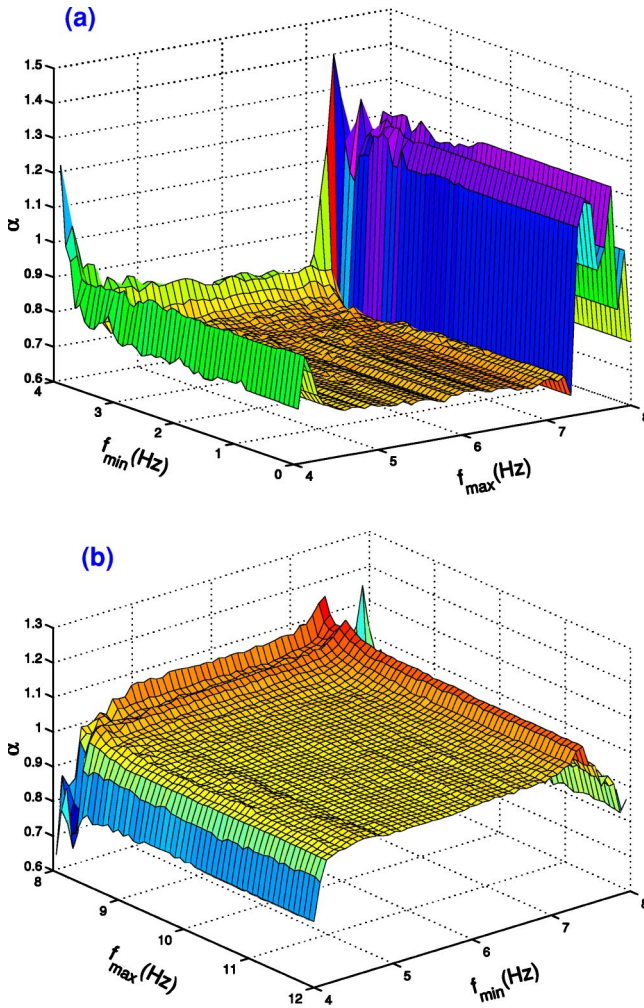
(a)

(b)

FIG. 5. Scaling exponent of the period dynamics of the decomposed first mode (a) and second mode (b), as a function of the filtering boundaries. The double-mode oscillator is filtered by a band, set with a lower limit f_{min} and an upper limit f_{max}. The double-mode oscillator is comprised of an oscillator with a central frequency at 4 Hz and a scaling exponent $\alpha = 0.7$ and a second oscillator with a central frequency at 8 Hz and a scaling exponent $\alpha = 1$. For each lower limit and upper limit of the filtering band, the decomposed subsignal is obtained. The scaling exponents of both oscillators are systematically restored (the flat plain), as long as the filtering boundaries are not too close to the oscillator frequencies themselves.

of the PPI series of the basic frequency. As can be expected, no additional scaling information exists in the harmonics and the full scaling properties can be extracted by study of the first mode alone.

Before moving on to demonstrate how this method can be applied, we note that while the simulation results indicate that one can use this method to distinguish between apparent harmonics and distinct oscillators, it will be important in the future to derive an analytical proof. An analytical derivation can help to identify any limitations of the method and complement the present findings.
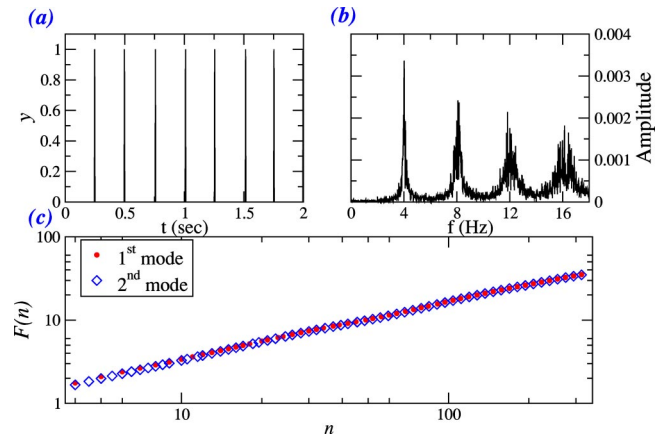

FIG. 6. (a) A pulse train signal with a time-dependent period that has scaling properties. (b) The respective power spectrum shows harmonic modes that are the effect of the nonlinearity of the signal. These modes were then filtered for peak detection. (c) The fluctuation functions of the period dynamics of the first two modes. The two curves coalesce, indicating that indeed no new information is hidden in the harmonics.

III. APPLICATION

We apply the technique to physiological data from patients with tremor from Parkinson's disease, a common, rhythmic movement disorder [26]. Patients were diagnosed according to United Kingdom Brain Bank criteria [27] by movement disorders experts at Tel-Aviv Sourasky Medical Center. Subjects were seated comfortably in a reclined chair with arms at rest, while combined registration of movement and muscle activity were performed. Surface electromyographic (EMG) recordings [28] were made from forearm flexor (EMG_{flex}) and extensor (EMG_{ext}) muscles, and movement was recorded on triaxial accelerometers (ACC) affixed to the dorsum of each hand. Data were recorded for multiple epochs of 10 min, and a total of 28 time series from ten patients were studied. We analyze the ACC measurements from the tremor predominant hand, and consider only the movement in the two directions transverse to the arm axis (the x axis), denoted as ACC_y and ACC_z. The anatomy and pathophysiology of this movement disorder causes hand tremor to be typically observed in the y and z directions, but not along the axis of the arm.

As already observed in previous studies [29,30], the main oscillation in parkinsonian tremor is around the frequencies of 4–5 Hz. The spectrum also shows peaks at roughly integer multiples of that fundamental frequency, for all patients (Fig. 1). However, we consider the possibility that although the peaks appear at the same frequencies as if they were pure harmonics of the basic frequency, rising from the nonlinearity of the signal, they may in fact represent independent modes of oscillation (i.e., perhaps independent oscillators give rise to these multiple frequencies). We analyze the first two modes, to see if it is possible to distinguish between them, based on their scaling exponents. Accordingly, the filtering band was taken to be 2.00–6.45 Hz for the first mode, and 6.67–10.00 Hz for the second mode (Fig. 7). To estimate the error of the applied filter, we calculated the ratio of the
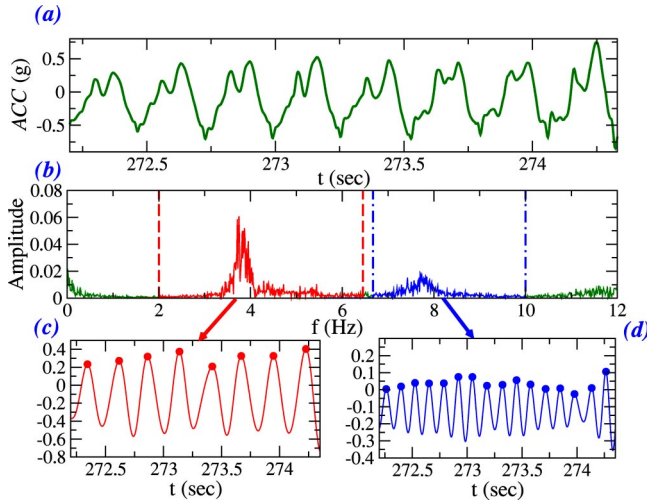
FIG. 7. Decomposition employed on tremor data. (a) A typical example of acceleration measurements from a patient with Parkinson's disease. (b) The respective power spectrum displays the two modes, around 4 Hz and 8 Hz. (c) The first mode signal obtained by filtering in the range 2.00–6.45 Hz. (d) The second mode signal obtained by filtering in the range 6.67–10.00 Hz.

areas under the filtered spectrum and the total spectrum. We found that for the simulated signal, 99.9% of the total area of the power spectrum was located inside the filter boundaries, indicating that any errors imposed by the method are quite small and are likely to have a negligible effect.

A. Results

After filtering, the PPI series are derived, and second order DFA [31] is performed to produce the fluctuation function which shows consistent long-term scaling at large scales. The scaling exponent α is estimated in the range of time scales n between 44 and 230 [25], to avoid small scale errors, as observed in the simulations [Fig. 3(c)], and finite-size effects [32]. We find that the periods in tremulous motion and muscle activity do not change randomly, but there exist long-range correlations. All measurements produce roughly the same mean value of α for the two modes (Table I).

Interestingly, there is, however, a dissimilarity between the supposedly harmonic modes. This finding raises the possibility that there are several distinct oscillators, instead of a

TABLE I. Mean values and standard deviation of the scaling exponent α for the period dynamics of the first two modes in hand acceleration and muscle activity patterns in patients with tremor predominant Parkinson's disease. ACC_y and ACC_z columns show the results for the oscillations in the y-and z-axis acceleration, respectively, while EMG_{flex} and EMG_{ext} columns show the results for the flexor and extensor muscles activity, respectively. Note that the mean value of α is similar in both modes for all measurements.

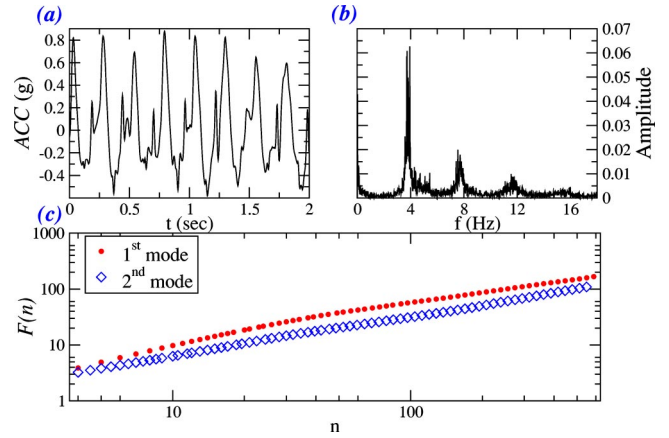|	ACC_y	ACC_z	EMG_{flex}	EMG_{ext}
First mode	0.8±0.11	0.81±0.12	0.72±0.13	0.75±0.13
Second mode	0.79±0.1	0.78±0.08	0.74±0.13	0.76±0.11

FIG. 8. (a) A typical example of an acceleration signal in tremor, and (b) its respective power spectrum. (c) The fluctuation functions of the period dynamics of the two modes do not overlap, suggesting that they are not simply harmonics generated by the nonlinearity of the signal (in contrast with Fig. 6).

single oscillator and harmonics. The fluctuation functions of different modes from both ACC and EMG data form distinct curves, suggesting that they are not simple harmonics of the fundamental frequency (Fig. 8), generated by one nonlinear oscillator (in contrast with Fig. 6). Therefore, the different patterns of the fluctuation function suggest that some tremor mechanism(s) generates more than one independent mode of oscillation that happens to appear in harmonic frequencies.

The scaling exponents from ACC and EMG data were then compared to determine the degree of the associations between them (using linear correlation coefficient [33]), both among the different moving directions—the transverse modes—and among the antagonistic muscle groups (Table II). It is notable that although the mean value of α is similar for both modes, there are also significant differences between the two modes.

B. Discussion

We relate the association between ACC_y and ACC_z, in both modes, to mechanical coupling. As a result of the inter-

TABLE II. Comparison of the linear correlation coefficients (r) for α's from different measurements in the same mode. The upper triangular above the diagonal in bold shows the correlation coefficients for the first mode, while the lower triangular below the diagonal shows the correlation coefficients for the second mode. A good correlation between the two. * denotes significant linear association. Note that the two modes are distinct from each other: whereas in the first mode there is no correlation between α's from muscle activity and the actual movement, in the second mode there is good correlation between the two.

	ACC_y	ACC_z	EMG_{flex}	EMG_{ext}
ACC_y		**0.8***	**0.14**	**0.13**
ACC_z	0.64*		**0.12**	**0.38**
EMG_{flex}	0.87*	0.66*		**0.02**
EMG_{ext}	0.76*	0.54*	0.77*	

action, the oscillations in both directions can become "mode locked," and thus become correlated with one another. Only in the second mode, however, there is a strong association between α's of the antagonistic muscle groups, and also between α's of EMG and ACC. In contrast, in the first mode, the association is very weak. It is reasonable to assume that the association between the acceleration and the muscle activity originates from the coordination of flexor and extensor muscles. Since movement is determined by the joint activity of flexor and extensor muscles, if there is a cross correlation between the muscles, there will also be a cross correlation between individual transverse mode accelerations and the individual muscle activities.

Evidently, although the mean values of α are very close in both modes, they are described by separate sets of behavior. Thus, it is likely that there exists more than one mode of oscillation. Central oscillations in the brain may account for the appearance of different modes of oscillation [34] and synchronized activity of cortical motor areas may determine the correspondence between the antagonistic muscles [35]. Further work is needed to determine why apparently independent tremor oscillations occur at integer multiples (e.g., 1:2 ratio). It is important to note, however, that this type of behavior is not so uncommon in physiology. For example, in primitive neural circuitry, e.g., in the lamprey, coupled, *independent* oscillators have been shown to be responsible for oscillations at integer multiples (i.e., at harmonic frequencies).

IV. SUMMARY

To summarize, we suggest that filtering in the frequency domain of multimodal signals with long-range memory in the period dynamics can preserve the long-range correlation properties of the period series. The validity of the filtering method is systematically tested on simulated signals with two modes of oscillation, with different configurations of generated correlated noise. We change the boundaries of the filtering range and show that the method is robust. The method can be used to distinguish between two possible mechanisms that generate an apparent harmonic structure, a nonlinear signal and multimodal (independent) oscillations. The first has only a single statistical origin, while the second may have multiple driving processes. Application of this method to parkinsonian tremor illustrates how our decomposition technique can be used to analyze the long-term scaling properties of semiperiodic signals with multiple dominant frequencies. Finally, we conclude that scaling analysis of the period dynamics of tremor suggests that the harmonic structure of tremor is likely the product of multimodal oscillations rather than simple harmonics of a nonlinear oscillation.

APPENDIX: SCALING

The dynamics of a stochastic series $\{\eta_i\}$ can be explored through its correlation properties, or in other words, the time ordering of the series. When there exist long-range temporal correlations, the autocorrelation function $C(n) \equiv \langle \eta_i \eta_{i+n} \rangle$, and the power spectrum $S(f)$ both exhibit a scaling behavior, $C(n) \sim n^{-\gamma}$ and $S(f) \sim f^{-\beta}$, where the scaling exponents β and γ are related by $\beta = 1 - \gamma$. Scaling can also be found in the fluctuation function of the series. DFA [22] is a technique that has been widely used to calculate the fluctuation function and avoid spurious detection of correlations that may be artifacts of nonstationarity. The DFA method consists of the following steps. We first integrate the $\{\eta_i\}$ series to construct the profile $Y(k) = \sum_{i=1}^{k} (\eta_i - \langle \eta \rangle)$ where $\langle \eta \rangle$ denotes the series average. Next, we divide the integrated signal, $Y(k)$, into equal nonoverlapping windows of size n and find the local trend in each window using a least-squares polynomial fit. The order of the polynomial fit specifies the order of the DFA. We then calculate the average of the square distances around the local trend. This procedure is repeated to obtain the root mean square fluctuation function $F(n)$ for different window sizes n. A power-law relation, $F(n) \sim n^{\alpha}$, indicates the presence of scaling in the series. The scaling exponent α is related to the other scaling exponents by $\alpha = 1 - \gamma/2 = (\beta + 1)/2$ [24]. The value $\alpha = 0.5$ indicates that there are no (or finite-range) correlations in the data. In contrast, the case of $\alpha > 0.5$ indicates the existence of long-term memory and scaling in the time series.

[1] W.H. Press, Comments. Astrophys. **7**, 103 (1978).

[2] J. Rhayem, M. Valenza, D. Rigaud, N. Szydlo, and H. Lebrun, J. Appl. Phys. **83**, 3660 (1998).

[3] N. Vandewalle, N. Ausloos, M. Houssa, P.W. Mertens, and M.M. Heyns, Appl. Phys. Lett. **74**, 1579 (1999).

[4] T. Gisiger, Biol. Rev. Camb. Philos. Soc. **76**, 161 (2001).

[5] A.L. Goldberger, D.R. Rigney, and B.J. West, Science **262**, 42 (1990).

[6] K. Linkenkaer-Hansen, V.V. Nikouline, J.M. Palva, and R.J. Ilomoniemi, Neuroscience **21**, 1370 (2001).

[7] E. Koscielny-Bunde, A. Bunde, S. Havlin, H.E. Roman, Y. Goldreich, and H.J. Schellnhuber, Phys. Rev. Lett. **81**, 729 (1998).

[8] Y. Liu, P. Gopikrishnan, P. Cizeau, M. Meyer, C.K. Peng, and H.E. Stanley, Phys. Rev. E **60**, 1390 (1999).

[9] R.N. Mantegna and H.E. Stanley, Nature (London) **376**, 46 (1995).

[10] P. Bak, *How Nature Works: The Science of Self-Organized Criticality* (Springer-Verlag, New York, 1996).

[11] J.B. Bassingthwaighte, L.S. Liebovitch, and B.J. West, *Fractal Physiology* (Oxford University Press, Oxford, 1994).

[12] B. Pilgram and D.T. Kaplan, Am. J. Physiol. **45**, 1 (1999).

[13] A.L. Goldberger, Lancet **347**, 1312 (1996).

[14] J.M. Hausdorff, C.K. Peng, Z. Ladin, J.Y. Wei, and A.L. Goldberger, J. Appl. Physiol. **78**, 349 (1995).

[15] S. Blesic, S. Milosevic, Dj. Stratimirovic, and M. Ljubisavljevic, Physica A **268**, 275 (1999).

[16] J. Timmer, M. Lauk, and G. Deuschl, Electromyogr. Motor C. **101**, 461 (1996).

[17] M. Gresty and D. Buckwell, J. Neurol., Neurosurg. Psychiatry **53**, 976 (1990).

[18] J.H. McAuley and C.D. Marsden, Brain **123**, 1545 (2000).

[19] C. De Boor, *A Practical Guide to Splines* (Springer-Verlag, New York, 1978).

[20] C.K. Peng, S. Havlin, M. Schwartz, and H.E. Stanley, Phys. Rev. A **44**, 2239 (1991).

[21] A. Papoulis, *Signal Analysis* (McGraw-Hill, New York, 1977).

[22] C.K. Peng, S.V. Buldyrev, S. Havlin, M. Simons, H.E. Stanley, and A.L. Goldberger, Phys. Rev. E **49**, 1685 (1994).

[23] A.L. Goldberger, L.A.N. Amaral, J.M. Hausdorff, P.Ch. Ivanov, C.-K. Peng, and H.E. Stanley, Proc. Natl. Acad. Sci. U.S.A. **99**, 2466 (2002).

[24] T. Vicsek, *Fractal Growth Phenomenon*, 2nd ed. (World Scientific, Singapore, 1993).

[25] The time scale of the fluctuation function for the second mode is divided by 2 (the harmonic number), to correspond with the one of the first modes.

[26] The data upon which we based our analysis will be available without charge for downloading from www.physionet.org

[27] A. Hughes, S. Daniel, L. Kilford, and A. Lees, J. Neurol., Neurosurg. Psychiatry **55**, 181 (1992).

[28] Prior to further analysis, EMG data for both muscle groups were rectified and filtered.

[29] S. Spieker, A. Boose, S. Breit, and J. Dichgans, Mov Disord. **13**, 81 (1998).

[30] J. Raethjen, M. Lindemann, H. Schmaljohann, R. Wenzelburger, G. Pfister, and G. Deuschl, Mov Disord. **15**, 84 (2000).

[31] A. Bunde, S. Havlin, J.W. Kantelhardt, T. Penzel, J.H. Peter, and K. Voigt, Phys. Rev. Lett. **85**, 3736 (2000).

[32] C.K. Peng, S.V. Buldyrev, A.L. Goldberger, S. Havlin, M. Simons, and H.E. Stanley, Phys. Rev. E **47**, 3730 (1993).

[33] W.H. Press, S.A. Teukolsky, W.T. Vetterling, and B.P. Flannery, *Numerical Recipes in C*, 2nd ed. (Cambridge University Press, Cambridge, 1996).

[34] M.R. Mehta and H. Bergman, J. Neurosci. Methods **62**, 65 (1995).

[35] P. Tass, M.G. Rosenblum, J. Weule, J. Kurths, A. Pikovsky, J. Volkmann, A. Schnitzler, and H.J. Freund, Phys. Rev. Lett. **81**, 3291 (1998).